CMOD5.H—A High Wind Geophysical Model Function for C-Band Vertically Polarized Satellite Scatterometer Measurements

Seubson Soisuvarn, *Member, IEEE*, Zorana Jelenak, *Member, IEEE*, Paul S. Chang, *Member, IEEE*, Suleiman O. Alsweiss, *Member, IEEE*, and Qi Zhu

***Abstract*—The Advanced Scatterometer (ASCAT) on the MetOp-A satellite is a radar instrument designed specifically to retrieve the ocean surface wind speed and direction. The ASCAT wind vector products are produced and utilized operationally in support of the National Oceanic and Atmospheric Administration (NOAA)'s weather forecasting and warning mission. The standard ASCAT winds at NOAA are produced using the ASCAT wind data processor developed at the Royal Netherlands Meteorological Institute (KNMI) utilizing the CMOD5.n geophysical model function (GMF). Recent validation of the ASCAT wind retrievals revealed a low bias at high wind speeds when compared to both the QuikSCAT winds and the National Centers for Environmental Prediction numerical weather prediction (NWP) model winds. The goal of this paper is to investigate the ASCAT high-wind-speed performance and to modify, as appropriate, the high-wind-speed portion of CMOD5.n GMF. This effort would potentially improve the utility of ASCAT wind retrievals in supporting wind warning and analysis and thus better mitigate the loss of QuikSCAT data products. Traditionally, the GMF is developed empirically by collocating scatterometer measurements and other truth data such as buoy and NWP model winds. However, NWP models are known to underestimate the intensity of higher wind speeds, and data sources such as ship-based or buoy-based observations provide an inadequate quantity of measurements for empirical GMF development. In this paper, a method utilizing aircraft-based scatterometer measurements in the high-wind-speed regimes is used in conjunction with satellite scatterometer measurements to refine the satellite GMF. As a result of this paper, a high wind C-band satellite GMF, CMOD5.h, was developed and implemented in NOAA's ASCAT processor. The validation comparison of the high wind and standard ASCAT wind products revealed 0.6-m/s reduction in the wind speed bias for winds greater than 15 m/s with respect to QuikSCAT, WindSat, and Step Frequency Microwave Radiometer high wind measurements.**

***Index Terms*—Advanced Scatterometer (ASCAT), geophysical model function (GMF), high winds, ocean vector winds, QuikSCAT.**

Manuscript received July 18, 2011; revised February 6, 2012 and July 20, 2012; accepted July 27, 2012. Date of publication November 22, 2012; date of current version May 16, 2013. The views expressed in this paper are those of the authors and must not be interpreted as those of National Oceanic and Atmospheric Administration or the U.S. Government.

The authors are with the Center for Satellite Applications and Research, National Environmental Satellite, Data, and Information Service, National Oceanic and Atmospheric Administration, Camp Springs, MD 20746 USA (e-mail: seubson.soisuvarn@noaa.gov).

Color versions of one or more of the figures in this paper are available online at http://ieeexplore.ieee.org.

Digital Object Identifier 10.1109/TGRS.2012.2219871

I. Introduction

THE Advanced Scatterometer (ASCAT) is a microwave radar instrument designed primarily to retrieve ocean surface vector winds (OSVW). The first of three ASCAT instruments is carried on the European Organization for the Exploitation of Meteorological Satellites (EUMETSAT) MetOp-A satellite, which was launched on October 19, 2006. ASCAT collects the ocean surface backscatter (σ_0) using a C-band vertically polarized radar with three fan beam antennas on the left-hand side and on the right-hand side of the satellite track resulting in two swaths approximately 550 km wide with an approximately 700-km nadir gap between them. The antennas are oriented at $\pm 45°$, $\pm 90°$, and $\pm 135°$ with respect to the satellite track for the fore-, mid-, and aft-beams, respectively, and the earth incidence angles (EIAs) vary across the swath from $\sim 35° - 65°$ for the fore- and aft-beams and $\sim 25° - 55°$ for the mid-beams [1].

A thorough calibration of the ASCAT backscatter was carried out by the EUMETSAT [2]. Two calibrated σ_0 level 1b (L1B) swath gridded standard products are produced by performing a spatial average of σ_0 along- and across-track using a 2-D Hamming window centered at every node resulting in σ_0 triplets (fore-, mid-, and aft-beams) of 50-km resolution on a 25-km grid spacing and 25-km resolution on 12.5-km grid spacing [3].

The 50- and 25-km L1B σ_0 products are converted to level 2 OSVW products at 50- and 25-km spatial resolution, utilizing the ASCAT wind data processor (AWDP) developed at the Royal Netherlands Meteorological Institute (KNMI) [4], [5]. The AWDP utilizes the CMOD5.n geophysical model function (GMF) which relates C-band vertically polarized ocean backscatter measurements to 10-m height equivalent neutral stability wind vectors. This GMF was originally derived using C-band vertically polarized scatterometer data from the European Remote Sensing (ERS)-1 and ERS-2 satellites [6]. However, a correction factor developed by KNMI was applied to CMOD5.n GMF to extend its usability to ASCAT data [6].

The National Oceanic and Atmospheric Administration (NOAA) adapted the AWDP to produce standard ASCAT vector winds to support NOAA's operational weather warning and forecasting requirements. A comprehensive validation conducted at NOAA shows that both the 50- and 25-km spatial resolution ASCAT winds are consistent with each other. However, the validation also shows that ASCAT wind speeds are biased low at wind speeds $> \sim 15$ m/s in comparison to both

the Ku-band QuikSCAT scatterometer wind retrievals and the Global Data Assimilation System (GDAS) numerical weather prediction (NWP) model winds [7].

A comparison of ASCAT σ_0 measurements with QuikSCAT wind retrievals at similar spatial scales revealed that, at higher wind speeds, ASCAT σ_0 still exhibits some sensitivity that is not being represented in the current CMOD5.n GMF. This suggests that an improved high-wind-speed GMF can be developed for ASCAT. Typically, a power law is used to model the sensitivity of GMFs at higher wind speeds [8]. However, in this paper, the high wind portion of the GMF for ASCAT is also determined with the aid of high-resolution aircraft scatterometer measurements [9].

It is worth noting that QuikSCAT wind retrievals that were compared with ASCAT σ_0 measurements occurred at high latitudes, and the rain-flagged wind retrievals were excluded in the comparisons. The high latitude collocations between ASCAT and QuikSCAT resulted in high wind comparisons in extratropical cyclones where rain is not a significant factor and high wind speeds occur over spatial scales larger than the satellite footprints.

In Section II, statistical and operational validation results of the standard ASCAT and QuikSCAT wind products carried out by NOAA's Center for Satellite Applications and Research (STAR) office and the National Weather Service (NWS) Ocean Prediction Center (OPC) and National Hurricane Center (NHC) are presented. These results served as the motivation for developing the modified high-wind-speed portion of CMOD5.n. In Section III, a detailed derivation of CMOD5.h is provided, followed by validation and performance evaluation of CMOD5.h using collocated QuikSCAT and WindSat wind speed retrievals, GPS dropsondes, and Stepped Frequency Microwave Radiometer (SFMR) winds in Section IV. Finally, a summary and a conclusion are presented in Section V.

II. Motivation

A. ASCAT Winds in NOAA Operations

The launch of ASCAT provided a new source of spaceborne remotely sensed near-surface ocean wind field observations in the large mostly data-sparse regions, within the NOAA's NWS waters of responsibility. NOAA receives three flavors of L1B data, which are the nonaveraged σ_0 measurements (the full-resolution data set), the σ_0's averaged over 50 km and sampled at 25 km, and the σ_0's averaged over 25 km and sampled at 12.5 km. These data are provided in 3-min increment granules to NOAA's server in Darmstadt, Germany, at EUMETSET within 135 min of observation. The NOAA ASCAT Ingest server then pushes the data to the operational processing system and the parallel research processing system setup at STAR. The NOAA ASCAT level 2 products are also produced in near real time (NRT) on the parallel research system at STAR for further product development and validation. The graphical products displaying the global ocean wind maps, tropical storm centered wind vectors, and the global wind ambiguities are displayed on STAR's Ocean Winds Team Web page. This site is updated on an hourly basis with any newly available data and can be found at http://manati.orbit.nesdis.noaa.gov/ascat/.

B. Operational Validation of ASCAT Winds at OPC

The NOAA OPC is an integral component of the National Centers for Environmental Prediction (NCEP) within the NWS and has the responsibility of issuing marine weather forecasts, wind warnings, and guidance in text and graphical format to maritime users in the northern Atlantic and Pacific. The OPC issues marine wind warnings in accordance to the international standards for marine weather services, established by the World Meteorological Organization. The OPC warnings are based upon the Beaufort wind speed scale [10] and fall into three categories: gale force (17–23.5 m/s), storm force (24–31.5 m/s), and hurricane force (HF) for wind speeds of 32 m/s or greater. The OPC regions of forecast responsibility are frequently subjected to powerful cold fronts, and a variety of extratropical cyclones, including the rapidly intensifying cyclones, made OPC forecasters rely heavily, and in some situations almost exclusively, upon satellite OSVW.

The high-quality wind data previously available from QuikSCAT and more recently from ASCAT have greatly aided the OPC forecasters in filling some of the immense data gaps between conventional observations during the preparation of their routine and severe weather analysis and warning. While the OPC forecasters have access to a variety of additional data sources, such as imagery from geostationary satellites and meteorological fields from operational NWP models, to aid in the preparation of marine wind analyses and forecasts, only the scatterometer data provide detailed information on actual wind field spatial structure associated with the oceanic weather systems. The operational validation of the ASCAT wind retrievals was carried out within OPC shortly after ASCAT data became available in their NCEP Advanced Weather Interactive Processing System data stations in June 2007 [11]. This study indicated that ASCAT does reliably retrieve low to moderate surface wind speeds up to 15 m/s in all weather conditions. This performance represents an improvement over QuikSCAT, which was more adversely impacted by rain. However, for higher wind speeds ($>$ 15 m/s), the ASCAT retrievals were biased low, with the bias increasing with increasing wind speed with respect to QuikSCAT.

A study conducted by OPC evaluating ASCAT utility for detecting HF warning capability revealed that about 98% of the HF wind events detected by QuikSCAT (Fig. 1) were either not observed or not retrieved by ASCAT. This is mainly attributed to the reduced swath coverage and the reduced high-wind-speed sensitivity of ASCAT. The reduction in ability to detect HF wind events impedes ASCAT's competence to support OPC's marine weather warning and forecasting mission in a similar way that QuikSCAT did. Any improvements in ASCAT's high wind retrieval performance would increase ASCAT's utility to OPC.

C. ASCAT Warning Utility at TAFB

OSVW retrievals from the ASCAT instrument have also been available in NRT in the operational workstations at the NHC since June 27, 2007. An operational evaluation of QuikSCAT and ASCAT data was conducted by forecasters in the NHC

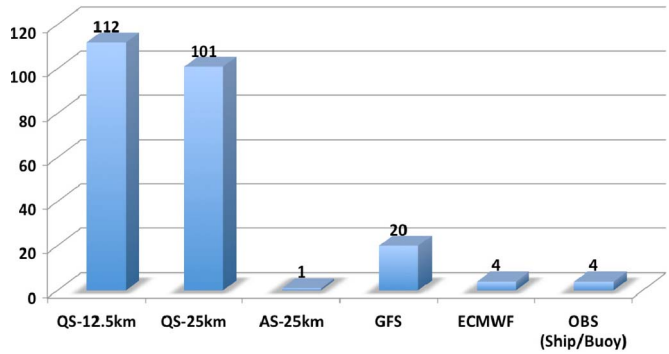

Fig. 1. Number of observations with HF winds in extratropical cyclones over the North Atlantic basin during the 2007–2008 cold season from the 12.5- and 25-km QuikSCAT wind products, 25-km ASCAT wind product, ship and buoy observations (OBS), GFS, and ECMWF 10-m NWP winds.

Tropical Analysis and Forecast Branch (TAFB) during the period from October 25, 2007, to February 8, 2008 [12]. The 25-km spatial resolution wind retrievals from ASCAT and QuikSCAT in the Gulf of Papagayo and Gulf of Tehuantepec were compared, and ASCAT winds averaged only 0.07 and 0.092 kts weaker, respectively. However, a closer look reveals that, while retrievals are quite comparable for winds up to $\sim$10 m/s, ASCAT winds are biased low compared to QuikSCAT for wind speeds above 10 m/s, and the bias is becoming much more apparent for winds above gale force strength ($>$ 17 m/s). The bias becomes larger when comparing the 12.5-km spatial resolution QuikSCAT winds to the 25-km spatial resolution ASCAT wind, which is perhaps not surprising. It is worth noting that there is no precipitation associated with these high-wind-speed events.

This negative wind speed bias was evident in the evaluation of ASCAT and QuikSCAT data over the Gulf of Tehuantepec during the 2007–2008 cool season strong wind events. There were a total of seven storm force wind events detected by the 12.5-km spatial resolution QuikSCAT wind retrievals. The 25-km spatial resolution ASCAT wind retrievals only captured one storm event with maximum winds of 25 m/s. The corresponding 12.5-km spatial resolution QuikSCAT data indicated HF winds of 35 m/s, corresponding to a 10-m/s difference and a different wind warning category [12].

D. ASCAT High Wind Validation with QuikSCAT and WindSat

It is very difficult to obtain high-quality *in situ* wind data in the high-wind-speed regimes. Winds measured by moored small-hulled buoys become increasingly low biased as wind speeds exceed 20 m/s [13]. Ordinary ship reported winds are of poor quality in this high-wind-speed range, and the better-equipped research vessels rarely sample this wind regime [14]. Finally, marine wind fields produced by NWP models, including even the products of the newer "reanalysis" projects, are notoriously biased low in severe storms [14], [15]. The best-suited candidates to assess the performance of new wind measurements are actually other spaceborne ocean wind vector instruments (such as QuikSCAT and WindSat), provided that their performance in high-wind-speed regimes is well understood.

1) QuikSCAT High Wind Measurements: The SeaWinds instrument onboard QuikSCAT is a Ku-band scatterometer designed by the Jet Propulsion Laboratory (JPL), National Aeronautics and Space Administration, to measure global OSVW. Over the course of the QuikSCAT mission (June 1999 to November 2009), JPL processed QuikSCAT wind products with three different GMF versions: QSCAT-1 [8], [16], QSCAT-2006 [17], and Ku-2011 [18]. The NOAA NRT retrieval algorithm utilized the QSCAT-1 GMF. After development of QSCAT-2006, NOAA did implement a parallel processing system to test and evaluate the QSCAT-2006 GMF. However, it was determined that the high-wind-speed modification of this GMF yielded winds that were too high, so the NOAA processing continued using the QSCAT-1 GMF. The Ku-2011 GMF, developed after QuikSCAT ceased nominal operations, has a high-wind-speed performance that lies between that of QSCAT-1 and QSCAT-2006. Since most of the high wind validation studies to date have utilized the QSCAT-1 QuikSCAT products, we also used these QuikSCAT products in our initial QuikSCAT–ASCAT assessment. However, our final analysis was done by utilizing newest remote sensing systems (RSS) QuikSCAT product processed with Ku-2011 GMF.

The QuikSCAT (QSCAT-1) winds have been extensively validated with NWP model analysis [19], buoy measurements [20], and research vessels [21]. Statistical comparisons of the wind vector components, direction and speed, show that the accuracies of QuikSCAT winds vary between 1.2–1.7 m/s for wind speed and 14–15° for wind direction for winds up to 20 m/s. The performance of high-wind-speed retrievals ($>$ 20 m/s) has proven to be highly dependent on whether a validation study was done in the tropical cyclone (TC) environments or elsewhere. The study that utilized collocated QuikSCAT measurements with GPS dropwindsondes deployed by the Dropwindsonde Observations for Typhoon Surveillance Near the Taiwan Region [22] experiment in 2003–2007 suggests a slight underestimation of the QuikSCAT wind speeds for tropical depression intensities (maximum 1-min 10-m wind less than 17.2 m/s) and finds a 4-m/s negative error bound in high wind regimes near TC intensities (maximum wind of 17.5–32.4 m/s). This is consistent with another study that compared the QuikSCAT wind retrieval performance relative to the NHC best track database. This study determined that the QuikSCAT wind retrievals do provide valuable information on the intensity of tropical depressions and tropical storms but not on the intensity of most hurricanes (wind speeds of 32.9 m/s or greater). Considering that the extreme winds in hurricanes occur at the much smaller spatial scales than the QuikSCAT sensor resolution and usually coincide with high rain events, we believe that the characterization of the QuikSCAT high-wind-speed performance on a global scale is not representative with these studies.

Cardone *et al.* [14] compared winds measured at the tops of drilling derricks at heights ranging from 80 to 140 m in the North Sea and Norwegian Sea with QuikSCAT winds for the period of July 1999 to December 2002. After reduction to a 10 m height and equivalent neutral conditions, it was found that, for the data comparisons of wind speeds greater than 20 m/s, the bias is -0.08 m/s; with QuikSCAT winds being lower than the platform winds, the standard deviation of the difference is 2.5 m/s, and the scatter index, expressed as a percentage, is

12%. The authors concluded that QuikSCAT wind data are useful and accurate to at least 35 m/s.

During the 2007 North Atlantic winter season, NOAA conducted an ocean wind experiment utilizing the NOAA N42RF WP-P3D aircraft [23] with the goal of characterizing the QuikSCAT high-wind-speed retrieval performance within the extratropical storm environment. Two flights into HF extratropical storms with winds $>$ 32 m/s on February 7 and 9 were coincident with QuikSCAT passes. During the February 7 flight, winds in excess of 40 m/s were observed over an area of 8643 km^2. Additionally, the high-wind-speed observations made during this flight were effectively rain-free. Surface wind speeds were measured by SFMR [24] as well as GPS dropsondes [25]. Subsequent analysis of the QuikSCAT retrievals showed high correlation with aircraft surface wind observations. QuikSCAT wind retrievals accurately depicted not just wind speed levels (up to 45 m/s) but also the extent of the high-wind-speed radius.

Yuan [26] validated QuikSCAT high-wind-speed observations ($>$ 20 m/s) in the Southern Hemisphere using weather station measurements and ECMWF fields. This study concluded that, while no systematic bias was found between *in situ* winds and satellite observations of high wind speeds, weather station winds and QuikSCAT winds were consistently higher than ECMWF winds at the same location within the high wind band.

These studies and experiments provide evidence that QuikSCAT wind retrievals within mid-latitude Northern and Southern Hemisphere storms are valid for wind speeds to at least 35 m/s. Based on these studies and forecaster experience with QuikSCAT high winds for wind and wave warning decisions, we conclude that QuikSCAT wind retrievals can be used as ground truth for ASCAT high wind validation analysis.

2) ASCAT QuikSCAT Comparisons: Initial statistical validation of the NOAA 25-km spatial resolution ASCAT wind product was accomplished by comparing it with the NCEP GDAS model wind field and the NESDIS NRT QuikSCAT 25-km spatial resolution wind product. A triple-collocation data set was constructed, and the performance of the ASCAT wind retrieval algorithm was assessed. A near coincident set of QuikSCAT winds was collected using a $\pm$1.5-h time window and a 25-km spatial window from the ASCAT observations for a period of one year, from January to December 2009. The collocated data set was flagged for rain using the QuikSCAT rain flag [27] and the ASCAT quality control flag [4]. The orbits of the two satellites resulted in a collocation database focused mainly in the high latitudes. Thus, the majority of the collocated high wind speeds were obtained in extratropical cyclones where rain tends to be less significant and high wind speeds occur over scales larger than the sensor spatial resolution. The NCEP GDAS model analysis provides wind vectors at 10 m height on a global $1^\circ \times 1^\circ$ grid four times a day at: 0000, 0600, 1200, and 1800 UTC. ASCAT wind measurements were collocated with GDAS model wind using trilinear space and time interpolations. The result of the ASCAT, QuikSCAT, and GDAS statistical wind speed analysis is shown in Fig. 2. The analysis shows that the QuikSCAT winds are higher than the GDAS model winds for wind speeds $>$ 15 m/s, while the ASCAT winds are lower. Considering that GDAS underestimate winds above the gale-force wind category (17.5 m/s) [15], the even lower ASCAT wind speed retrievals do hinder its utility in supporting NWS operational forecasting and warning products and services. However, ASCAT directional retrievals outperformed QuikSCAT for all wind speed ranges. This study was repeated using one year JPL QuikSCAT (Ku-2006 GMF [17]) and RSS QuikSCAT (Ku-2011) 25-km spatial resolution wind products collocated with ASCAT, and the results of these studies led to similar conclusion.

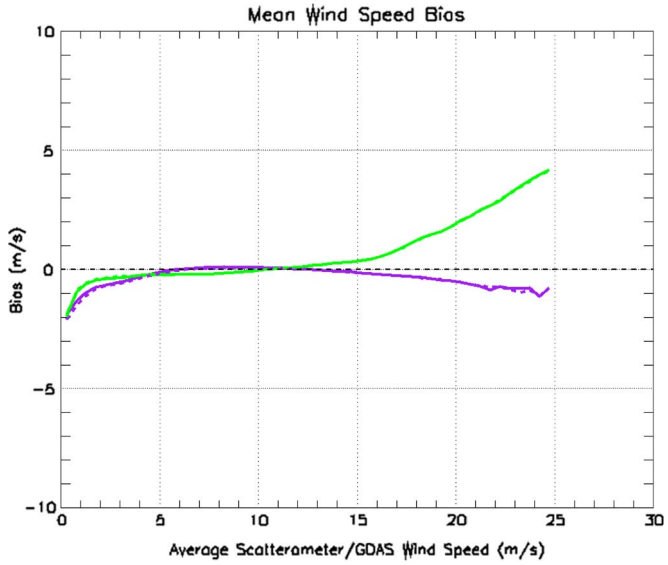

Fig. 2. Mean wind speed bias for two standard ASCAT products 25 km (purple solid line) and 12.5 km (purple dashed line) and two operational QuikSCAT products 25 km (green solid line) and 12.5 km (green dashed line) versus GDAS model winds.

Two more studies validated ASCAT winds with QuikSCAT [28], [29]. Similar to our study, Bentamy *et al.* found that the discrepancy between ASCAT and JPL QuikSCAT winds starts at 15 m/s. Patoux conducted combined analysis of ASCAT and JPL QuikSCAT ocean surface wind vector measurements using buoy measurements, NWP model analyses, and spectral decomposition. While this analysis reveals significant statistical differences between the two data sets, it concludes that JPL QuikSCAT wind speeds agree better with buoy wind speeds than ASCAT above 15 m/s and that ASCAT wind directions have overall better agreement with buoy directions than QuikSCAT. These findings are consistent with our ASCAT-QuikSCAT-GDAS comparisons (Fig. 2).

3) ASCAT WindSat Comparisons: WindSat is the first spaceborne fully polarimetric microwave radiometer, specifically designed to demonstrate the capability of retrieving OSVW from space using such a sensor. WindSat was launched on the Coriolis satellite on January 6, 2003, and it is still operating nominally. RSS developed an all-weather wind speed algorithm for the WindSat instrument [30]. The high-wind-speed validation of the RSS WindSat all-weather wind speed retrievals shows that these winds are accurate up to at least 35 m/s [31]. The WindSat 25-km gridded maps for eight environmental parameters including all-weather wind speed were released to the public on RSS website (www.remss.com) in April 2011.

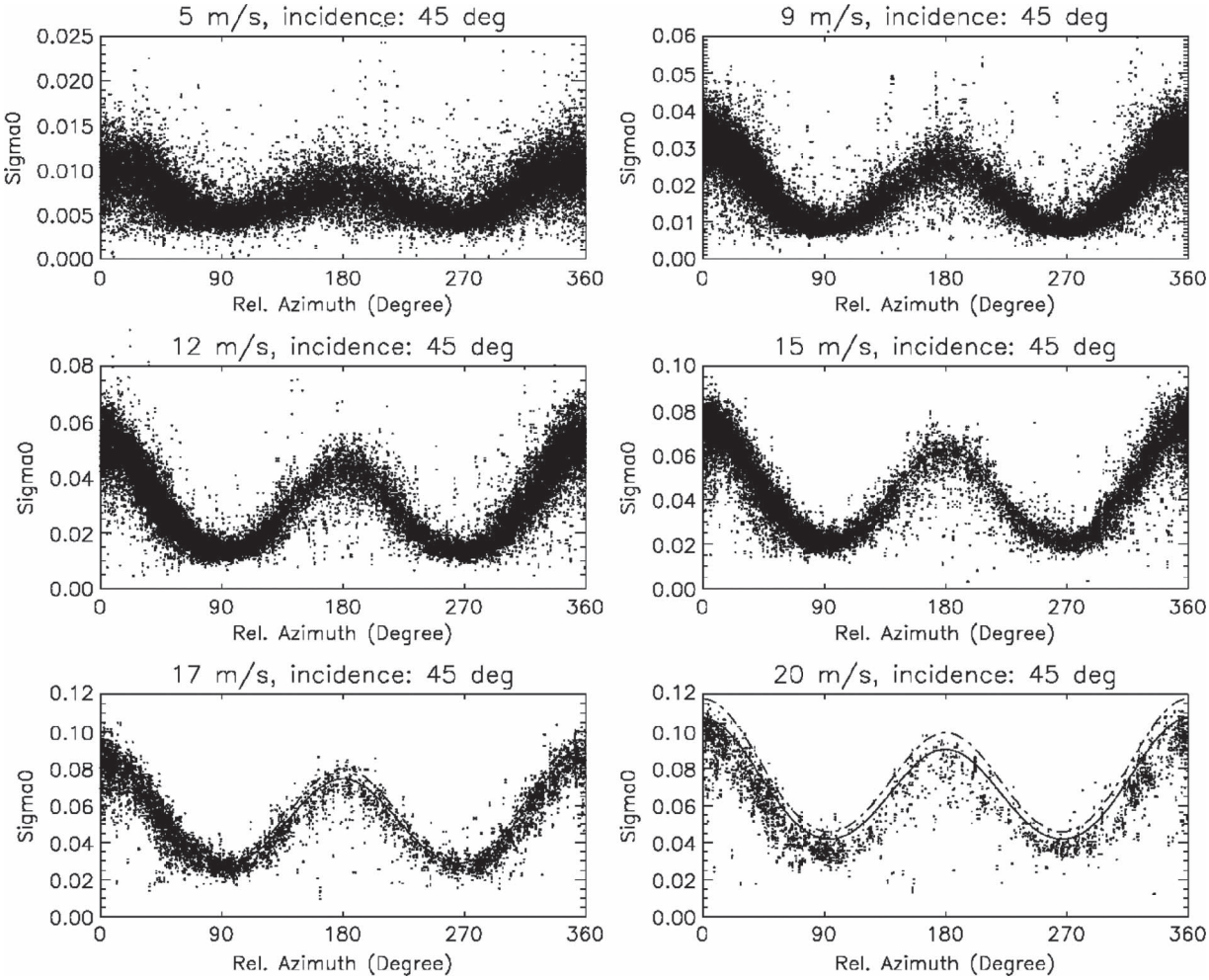

Fig. 3. Model function curve fit to the ASCAT σ_0 measurements at 45° incidence angle. The solid curves represent the CMOD5.h, and the dash-dot curves represent the CMOD5.n.

The WindSat and ASCAT measurements for the period between January and December 2008 were collocated. Due to differences in the WindSat and ASCAT orbits, the time window had to be extended to ± 3.0 h in order to obtain enough global collocations for a valid statistical analysis. As with the ASCAT-QuikSCAT collocations, a 25-km spatial window was utilized. Results from the WindSat–ASCAT validations (not shown here) are very similar to those of QuikSCAT–ASCAT, confirming a very good agreement between the two sensors for winds < 15 m/s with a departure in agreement thereafter.

The statistical results with QuikSCAT and WindSat are consistent with the operational validation results from OPC [11] and TAFB [12]. The question then became, could the ASCAT high wind retrievals be improved? The statistical analysis showed that ASCAT wind retrievals above 15 m/s are low compared to QuikSCAT, GDAS, and buoys. However, if ASCAT σ_0 measurements exhibit sensitivity at winds greater than 15 m/s that was not being characterized by the current ASCAT GMF, then there would be a possibility for improvement. Using collocated QuikSCAT and ASCAT measurements separated into 1-m/s wind speed bins and 2° EIA bins, we fitted ASCAT σ_0 with a double cosine function shown in (1). Statistical analysis of QuikSCAT wind retrievals and ASCAT σ_0 measurements does indeed show sensitivity in the ASCAT σ_0 measurements for winds greater than 15 m/s that is not being characterized by the current ASCAT GMF as shown in Figs. 3 and 4. A point-by-point comparison between the measured and modeled σ_0's for the left fore-, mid-, and aft-beams revealed gradual deviation of CMOD5.n from measurements starting at around the ~ -15 dB. The ASCAT backscatter measurements were collocated and matched to the 10-m neutral wind data from the 25-km NRT NOAA QuikSCAT wind vector product [32]. The ASCAT modeled backscatter values were calculated using the QuikSCAT winds and CMOD5.n GMF. The KNMI backscatter bias correction was applied to the measured ASCAT backscatter data to align it with CMOD5.n [6]. The comparison results between the measured and modeled σ_0's are shown in Figs. 3 and [4], where the ASCAT backscatter measurements are represented by black dots and the ASCAT modeled backscatter values are represented by dot-dashed line. Fig. 3 shows that both the measured and modeled ASCATs are in agreement up to 10 m/s, while the functional modulation determined by the B_1 and B_2 terms provides adequate fit to the data for all wind speeds. For winds higher than 10 m/s, the modeled backscatter is biased high relative to ASCAT backscatter measurements (Fig. 4), which indicates that there is additional wind speed sensitivity in the ASCAT backscatter measurements that is not being represented in the CMOD5.n GMF.

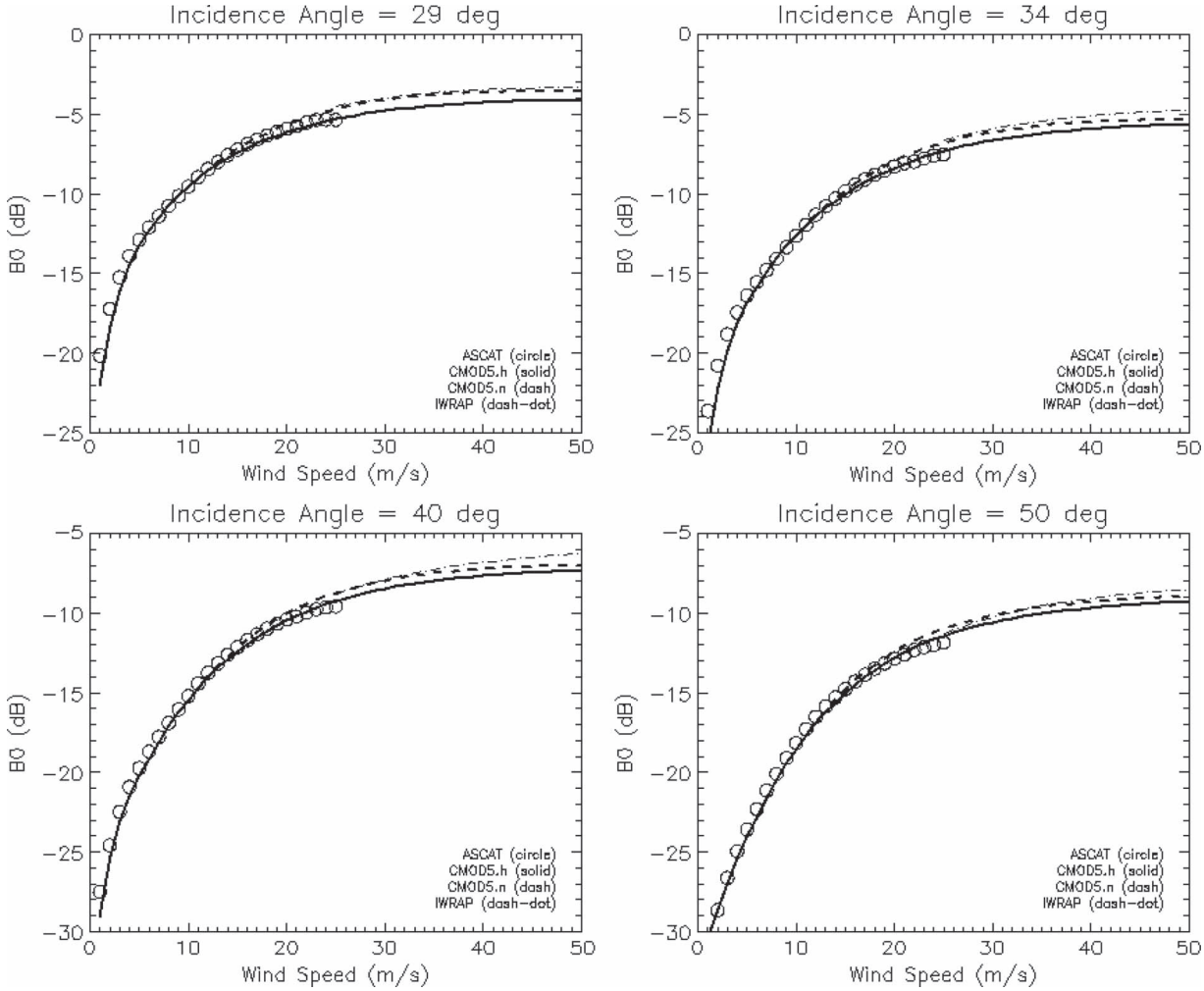

Fig. 4. Comparison of model B_0 from CMOD5.h, CMOD5.n, and IWRAP, and B_0 computed from ASCAT backscatter measurements as a function of averaged wind speed at 29, 34, 40, and 50° EIAs.

In the following sections, a new high-wind-speed ASCAT GMF is developed by utilizing QuikSCAT wind retrievals and C-band aircraft scatterometer measurements.

III. High-Wind-Speed Vertically Polarized C-Band GMF

A. CMOD5.n GMF

The initial development of the C-band V-pol GMF (CMOD) was instigated by the development of the C-band AMI scatterometer, which was launched in 1991, onboard the ERS-1 satellite, by the European Space Agency. The prelaunch model function, CMOD2 [33], was based on data collected from airborne campaigns. Soon after the launch of ERS-1, it was shown that CMOD2 was inadequate, and a replacement GMF, called CMOD4, was developed [34] using actual ERS-1 measurements. The CMOD4 relates the backscatter to neutral winds at 10 m height and was applicable for EIA ranges between 18° and 55°.

All CMOD models utilize an empirical functional relationship between normalized backscatter σ_0, 10-m-height wind speed v, wind direction relative to the antenna azimuth look direction (both measured from the North) $\emptyset$, and incidence angle θ and are of the form

$$\sigma_0(\theta, v, \emptyset) = B_0(\theta, v).[1 + B_1(\theta, v)\cos(\emptyset) + B_2(\theta, v)\cos(2\emptyset)]^p. \quad (1)$$

The three B_i terms shape the model's wind speed and directional dependence and are empirically derived along with the factor p. Moreover, while all three B_i terms have some wind speed dependence, the dominant wind speed dependence is captured in the B_0 term. The wind direction dependence is characterized by the two harmonic terms B_1 and B_2. The B_2 term describes the upwind–crosswind asymmetry and is used to determine the wind flow direction, while the B_1 term describes the upwind–downwind difference. The parameter p is set to 1.6 and effectively avoids the need in (1) to consider higher harmonics.

Subsequent analysis of ERS-1 and ERS-2 wind retrievals using the CMOD4 model function has shown a negative wind speed bias compared to the ECMWF winds. This can be largely attributed to nonoptimal description of the B_0 term. However, there was independent evidence from field experiments [9, 35, 36] that also showed inadequacies in the formulation of the B_1 and B_2 terms in very high winds. This led to

development of the CMOD5 model [37]. The CMOD5 GMF was derived from the analysis of collocated ERS-2 AMI σ_0 measurements and ECMWF short-range forecast winds. The CMOD5 GMF yielded a more uniform wind vector retrieval performance across the AMI swath. The CMOD5 GMF also extended the wind speed range for C-band scatterometers from 24 to 35 m/s [38]. However, subsequent studies using triple collocation with buoys [37], [39], [40] revealed a negative bias of around 0.50 m/s, which led to the development of the CMOD5.n GMF with an enhancement of 0.7 m/s in wind speed [41]. The value of 0.7 m/s was chosen to be independent of wind speed and incidence angle and accounted for the average difference between neutral and nonneutral winds (0.2 m/s) in addition to the 0.5-m/s negative bias.

The CMOD5.n GMF has been empirically extended to the ASCAT incidence angles 26°–66° and implemented in the AWDP developed by KNMI. Differences in ASCAT and AMI calibrations required implementation of an additional bias correction in AWDP to utilize CMOD5.n [6]. The bias correction factors are similar for each of the ASCAT antenna beams and are a function of incidence angle.

B. Airborne High-Wind-Speed GMF

Fine spatial resolution σ_0 measurements were collected at very high wind speeds (25–65 m/s) with the University of Massachusetts' Imaging Wind and Rain Airborne Profiler (IWRAP) during the 2002 and 2003 hurricane seasons. The IWRAP is a conically scanning dual-polarized (HH and VV polarizations) dual-frequency (C- and Ku-band) airborne Doppler radar that measures the Doppler velocity and reflectivity profiles from precipitation at 15–150-m resolution as well as the ocean surface backscatter, simultaneously at up to four different incidence angles (approximately 30°, 35°, 40°, and 50°) [42]. At a nominal conical scanning rate of 60 r/min, IWRAP measures the full azimuthal backscatter response at four incidence angles, two frequencies, and two polarizations every second [9]. From the flight level wind direction, onboard coincident SFMR wind speed estimates and GPS dropsonde measurements, high wind Ku-band and C-band V-pol and H-pol GMFs were empirically derived by utilizing a Fourier cosine series form [9]

$$\sigma_0(\theta, v, \emptyset) = A_0(\theta, v).\left[1 + A_1(\theta, v)\cos(\emptyset) + A_2(\theta, v)\cos(2\emptyset)\right]. \quad (2)$$

The ocean backscatter observations clearly show departure from the power law relationship adopted in the CMOD4 GMF series, with a decreased sensitivity at high wind speeds and saturation for winds exceeding approximately 40 m/s. According to [9], to permit a slow roll-off departure from the conventional power law, it was sufficient to add an additional term at C-band, which resulted in a parabolic fitting, where both the wind speed and the A_0 term are expressed in a logarithmic scale. Therefore, the A_0 term for C-band high wind speed was described by

$$A_0(v) = 10.\left[\beta + \gamma_1 \log_{10} v + \gamma_2 \left(\log_{10}(v)\right)^2\right] \quad (3)$$

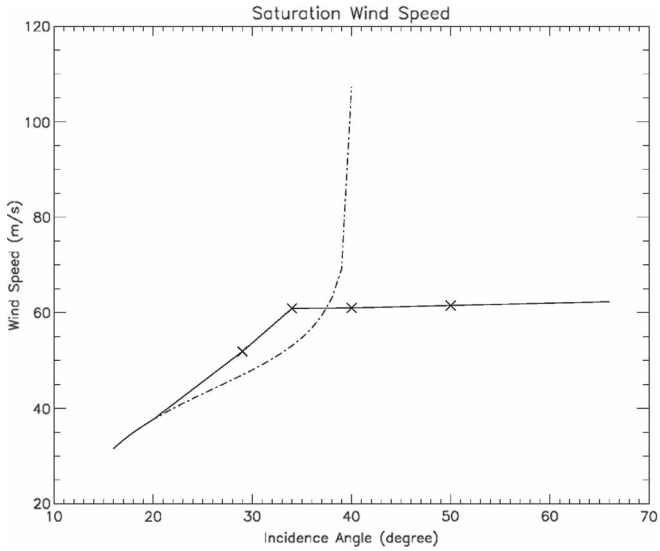

Fig. 5. Saturation wind speed as a function of incidence angles. The dash-dot line represents saturation wind speed of CMOD5.n GMF, and the solid line represents interpolation and extrapolation of the new saturation wind speed in the CMOD5.h. The X symbols represent saturation wind speeds for C-band V-pol IWRAP GMF.

where β, γ_1, and γ_2 coefficients are a function of incidence angle. The saturation wind speed $\nu_{\rm sat}$ is the point where A_0 reaches its maximum value, which can be determined as the zero of the first derivative of (3):

$$\left.\frac{\partial A_0(v)}{\partial \log_{10}(v)}\right|_{v=v_{\rm sat}} = 10.\left[\gamma_1 + 2\gamma_2 \log_{10}(v_{\rm sat})\right] = 0. \quad (4)$$

Note that the partial derivative of A_0 in (4) is a linear function of log wind speed. This attribute will be used to determine a new CMOD5.n B_0 term at high wind speeds in the following section.

The saturation wind speeds for vertically polarized C-band as a function of incidence angle are shown in Fig. 5. The X symbols represent IWRAP GMF saturation wind speeds of 51.9, 60.9, 61.0, and 61.5 m/s at 29°, 34°, 40°, and 50° incidence angles, respectively, as documented by [9]. The corresponding saturation wind speeds derived from CMOD5.n are shown as a dash-dot line in Fig. 5. Note that, for incidence angles $< 38°$, CMOD5.n and IWRAP models are generally in good agreement. At incidence angles around 38°–40°, CMOD5.n saturation wind speed sharply deviates from that of the IWRAP GMF and does not show any saturation for incidence angles $> 40°$. This trend suggests a deficiency in the CMOD5.n GMF for high wind speeds particularly at the higher incidence angles. Assuming that the airborne saturation wind speeds at 29°, 34°, 40°, and 50° incidence and the saturation wind speeds from CMOD5.n for 16°–20° incidence angles are correct, the extension for the entire ASCAT incidence angle range can be obtained by interpolation (shown as a solid line in Fig. 5).

The IWRAP model function was directly compared with CMOD5.n and ASCAT σ_0 measurements as shown in Fig. 4. The data analysis at high winds shows offset of 0.5-1 dB between IWRAP model and CMOD5.n (Fig. 4). Thus, implementing the high-wind-speed IWRAP GMF directly in the ASCAT wind retrieval processor directly would result in even

lower wind speed retrievals. This offset is probably partly due to the spatial resolution differences between the aircraft and satellite instrument footprints [43] and possibly residual errors in the IWRAP absolute calibration.

C. Derivation of New B_o Term

The main challenge in deriving high wind model function lies in obtaining a sufficient number of high-wind-speed collocations over the full range of wind directions to allow for a statistically robust empirical derivation of the GMF. Utilizing high-wind-speed QuikSCAT collocations would permit empirical derivation of the GMF for wind speeds up to 20–25 m/s. Rather than just extrapolating the GMF for winds greater than 25 m/s, we opted to combine additional sensitivity of ASCAT σ_0 revealed through comparison with QuikSCAT, with the high wind IWRAP GMF wind speed trend, while imposing the following conditions on the wind retrieval performance.

1) Wind vector retrieval performance below 10 m/s must not be degraded.
2) Directional retrieval accuracy should be preserved for all wind speed ranges.
3) The average gale force (17.5 m/s) and storm force (34 m/s) wind radii in extratropical storms should not extend beyond 300 or 600 km radius, respectively.

Following these conditions for moderate to high winds, the B_0 term was determined by examining the IWRAP GMF A_0 term dependence and by adjusting the B_0 values so that they satisfy the following properties: 1) the derivative of B_0 at high-wind-speed range is a linear function of the log wind speed, and 2) the saturation wind speed follows the solid line shown in Fig. 5.

The derivation of the new B_0 term was carried out in two steps: first, the derivative at a fixed incidence angle was defined as a linear function of the log wind speed $x = \log_{10}(\nu)$ in the form

$$\partial B_{0\text{new}}(x) = m.x + c = y \tag{5}$$

where the slope m and the constant c are unknowns. Given x and y, the slope m can be calculated from the expression

$$m = \frac{y_1 - y_2}{x_1 - x_2} \tag{6}$$

where x_2 is the log saturation wind speed $\log_{10}(\nu_{\text{sat}})$ and, thus, the corresponding $y_2 = 0$. Since CMOD5.n starts deviating from the ASCAT data at 10 m/s, it is reasonable to choose $x_1 = 1\ \log_{10}(10\ \text{m/s})$ as a starting wind speed and the corresponding $y_1 = \partial B_0(x_1 = 1)$. By substituting x and y values in (6), the slope m and the constant c can be determined:

$$m = \frac{\partial B_0(1)}{1 - \log_{10}(v_{\text{sat}})} \tag{7}$$

$$c = 0.5.\partial B_0(1)\left[1 - \frac{1 + \log_{10}(v_{\text{sat}})}{1 - \log_{10}(v_{\text{sat}})}\right]. \tag{8}$$

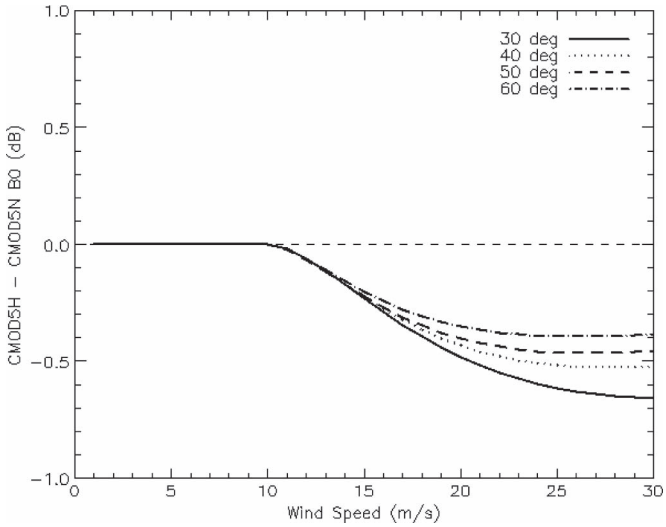

Fig. 6. CMOD5.h and CMOD5.n difference as a function of wind speed for different incidence angles.

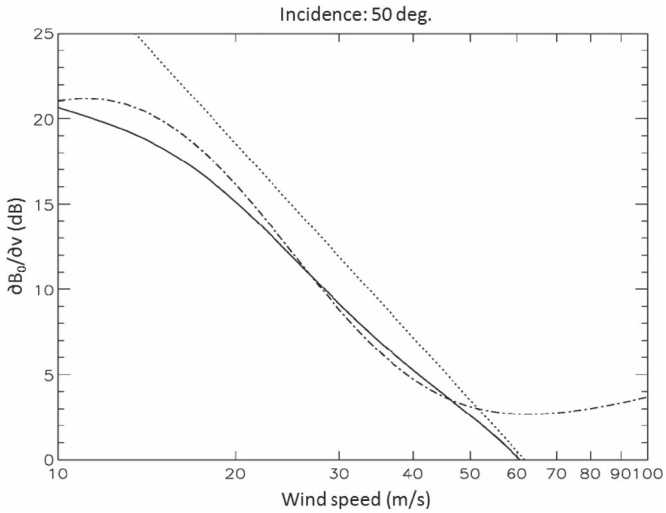

Fig. 7. First-order derivative of B_0 term as a function of wind speed in a log scale at 50° incidence angle. The new B_0 (solid) is mapped to approximately linear and saturated about IWRAP GMF (dotted) saturation wind speed, while CMOD5.n is shown in dash-dotted curve.

CMOD5.n is utilized in AWDP in tabulated form with 0.2-m/s wind speed steps and 1.0° incidence angle steps. To ensure continuity around 10 m/s and easy application of CMOD5.h in AWDP, the new B_0 was computed with the same wind speed and incidence angle steps, and the final revised B_0 was derived by normalizing the original B_0 as shown in the expression

$$B_{0\text{new}}(\theta, v) = B_0(\theta, v) \cdot \left[\frac{\sum_{n=1}^{N} \partial B_{0\text{new}}(x_n)}{\sum_{n=1}^{N} \partial B_0(x_n)}\right] \tag{9}$$

where N is equal 250, the total number of 0.2 m/s wind speed bins between 0.2 and 50.0 m/s. Since the incidence angle θ in (9) is considered a constant, the same procedure is repeated for the incidence angle bins of 1.0° between 16° and 66° to complete the lookup table for the new B_0.

The difference between CMOD5.h and CMOD5.n B_0 as a function of wind speed for four different incidence angles is shown in Fig. 6. The difference between the two models

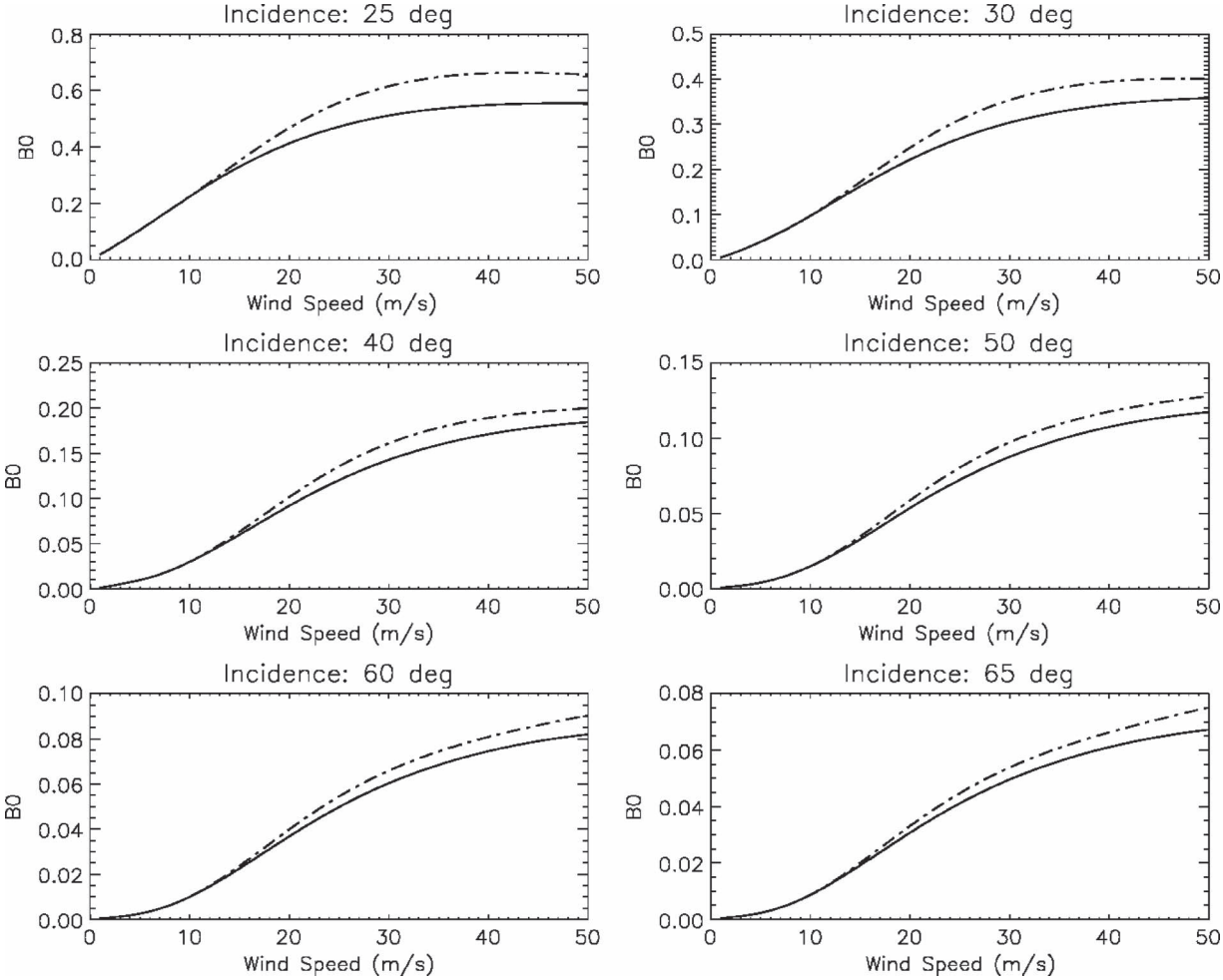

Fig. 8. Final B_0 coefficients as a function of wind speed up to 50 m/s for various incidence angles. The new B_0 is shown in a solid curve, and the original B_0 is shown in dash-dot curve.

decreases as the incidence angle increases, and it spans the range between -0.7 and -0.4 dB between the inner and outer ASCAT incidence angles. The differences between CMOD5.n and CMOD5.h are on the order of 0.2 dB for wind speeds around 15 m/s for all incidence angles, and they range from -0.6 dB at 30° incidence to 0.4 dB at 60° for wind speeds $\geq$ 25 m/s.

The derivatives of the original B_0 (dash-dot line), the new B_0 (solid line), and the IWRAP A_0 (dotted line) with respect to the log wind speed at 50° incidence angle are shown in Fig. 7. Both the new B_0 and IWRAP A_0 have a linear behavior with wind speed for speeds $> \sim$20 m/s and approach zero at the saturation wind speed of 61.5 m/s. The derivative of the original B_0 has a nonlinear trend with wind speed, with no apparent saturation wind speed, which is unrealistic.

In Fig. 8, the original B_0 and the new B_0 are plotted as a function of wind speed for various incidence angles. Both B_0 terms for wind speeds $<$ 10 m/s are identical as expected, but for wind speeds $> \sim$10 m/s, the new B_0 term is lower than the original B_0 term, which will result in higher wind speed retrievals given the same backscatter measurement.

Our assumption was that directional dependence shaped by B_1 and B_2 coefficients in CMOD5.n is valid for all wind speeds and should not be altered. To preserve the original B_1 and B_2 wind speed and directional dependence in (1), the new terms $B^h_{1,2}$ are defined by the following expression:

$$B^h_{1,2} = \left(\frac{B_0}{B^h_0}\right)^{\frac{1}{p}} B_{1,2}. \tag{10}$$

Fig. 9 visually shows the differences between the final CMOD5.h GMF when only a new B^h_0 is implemented and when all three terms are implemented. The overall change is small, but implementing the changes in the B_1 and B_2 terms ensures directional retrieval consistency with CMOD5.n.

IV. Wind Retrieval Validation

A. Comparisons With QuikSCAT and WindSat Winds

The comparisons of ASCAT with QuikSCAT and WindSat were done using one year (January to December 2008) of collocated wind vector retrievals produced by CMOD5.n and CMOD5.h (Fig. 10). Three different QuikSCAT products were used for analysis: RSS, JPL, and NOAA NRT QuikSCAT wind data. The results of this analysis are presented in Table I. As in [44], we assumed that errors are due to both ASCAT and

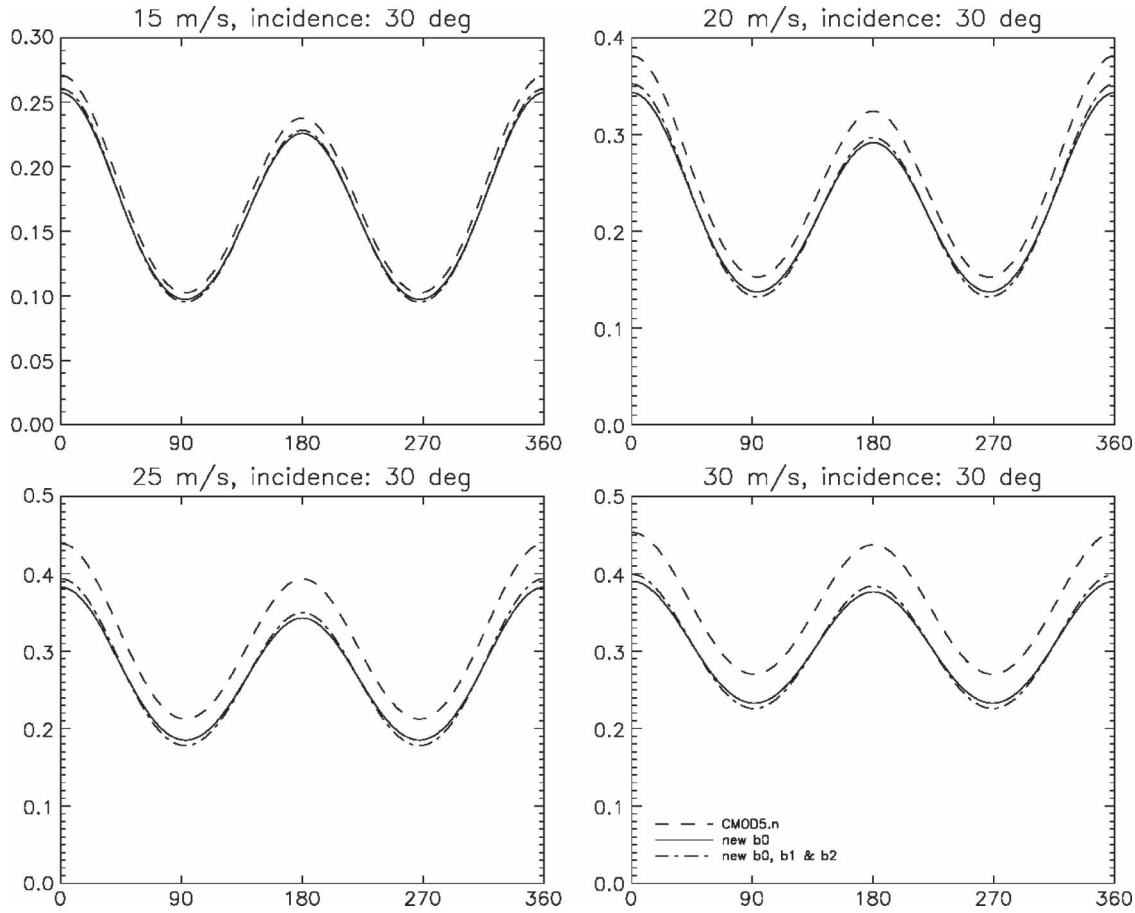

Fig. 9. Comparison of CMOD5.n (dash) and CMOD5.h with only new B_0 (solid) and CMOD5.h with all new B_0, B_1, and B_2 (dash-dot).

QuikSCAT or WindSat products and that the average wind speed from both is closest to the true average wind at the scatterometer scales. The data sets used in the analysis were filtered for rain as well as for large directional errors. Depending upon the wind field used for initialization of the ambiguity removal process, the ambiguity removal, and rain impact or spatial and time mismatch, directional errors between retrievals can be quite large. To eliminate this source of error, we filtered out all data that had directional differences $> 90°$; this filtering removed $\sim$3% of the data used in the analysis.

We found that, for winds up to 10 m/s, there is no difference between the standard or high wind ASCAT wind retrievals. This is expected since CMOD5.n and CMOD5.h are identical up to 10 m/s. For winds $>$ 15 m/s, the bias between the high wind ASCAT product and all data sets used in this analysis was reduced by about 0.6 m/s, while the standard deviations remained the same, ranging between 1.74 and 2.48 m/s, with respect to standard ASCAT product. The regime between 10 and 15 m/s is where the CMOD5.h was fitted to connect the high wind regime ($>$ 15 m/s) and the low wind regime ($<$ 10 m/s). We find slight degradation of 0.1 m/s in the bias error and 0.03 m/s in the standard deviation with respect to the QuikSCAT and WindSat wind data. As expected, the results show almost no difference in directional errors between the two ASCAT products, which is aligned with the constraint imposed on CMOD5.h in Section III.

B. Comparisons With SFMR and GPS Dropsonde Winds

During the 2010 Ocean Winds Winter Experiment, NOAA WP-D3 aircraft conducted four flights into extratropical storms coincident with ASCAT overpasses. The surface wind speeds were measured from the aircraft by SFMR and GPS dropsondes. A complete description of GPS dropsondes is given by [25]. An error analysis of the GPS sondes wind data by [25] indicates that the precision of the wind observations is $\sim$0.2 m/s, with an absolute accuracy of 0.5–2.0 m/s.

The GPS dropsondes were reprocessed using the ASPEN software to obtain the 10-m neutral stability winds, which were then collocated with ASCAT data. Time and spatial collocation constraints were set to 1 h and 5 km, respectively. During these four flights, 23 GPS sondes were deployed. Out of those 23 sondes, three measurements were discarded since measurements were taken in very unstable environment and large differences between GPS sonde and SFMR retrievals were found. Measured wind speeds spanned between 15 and 35 m/s as shown in Fig. 11(a) and (b). The bias between the dropsonde winds and the standard and high wind ASCAT winds was 1.37–0.57 m/s, respectively, while the standard deviation was 1.81–1.72 m/s, respectively. The directional scatter plot between ASCAT and GPS sonde wind directions is shown in Fig. 12, where only high wind ASCAT directions are presented because no differences were found between the two ASCAT wind products for lower winds speeds.

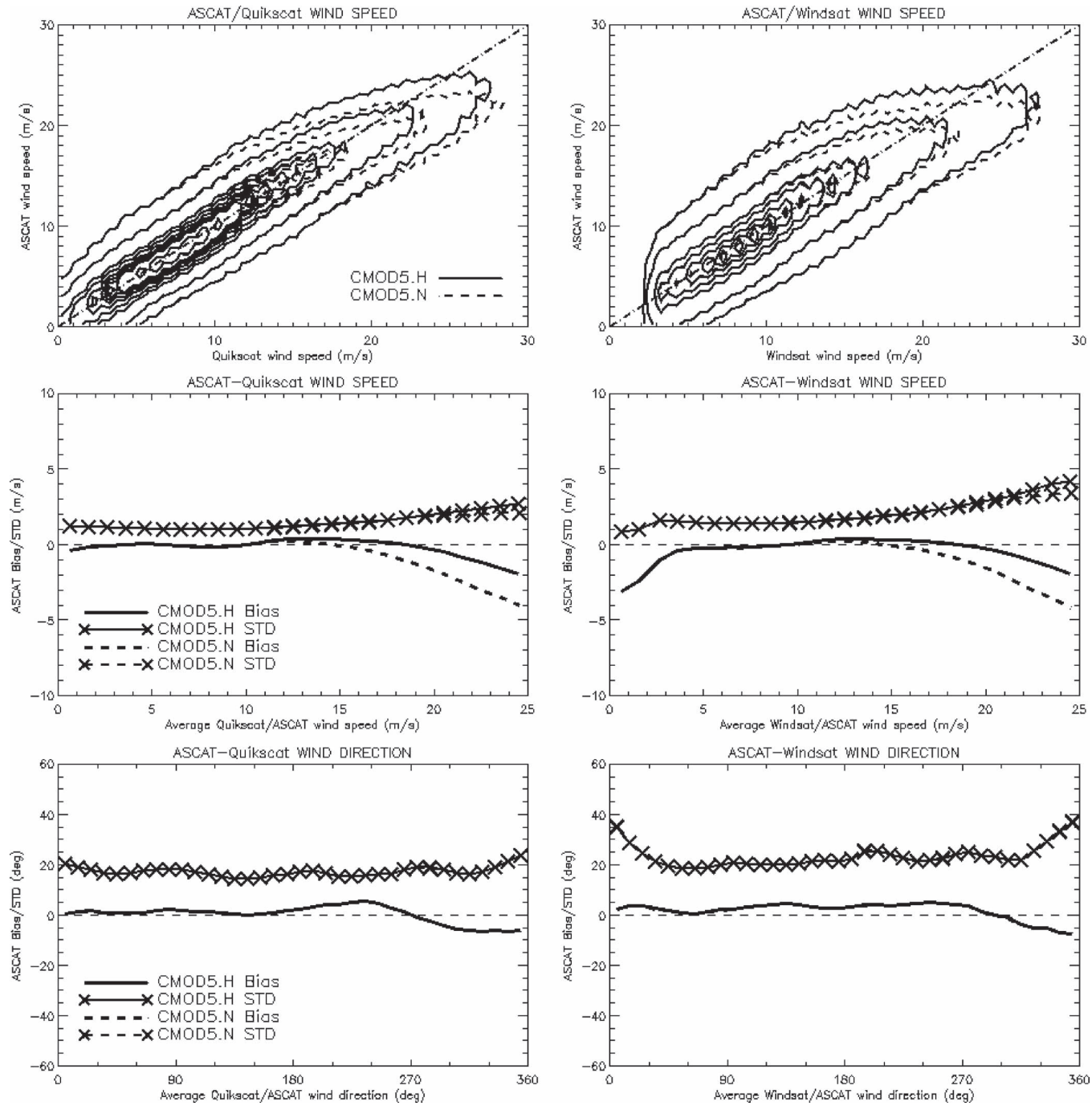

Fig. 10. ASCAT comparison with QuikSCAT (first column) and WindSat (second column). The contours represent relative density of data points (first row). The wind speed bias and STD difference, and wind direction bias and STD difference as a function of the averaged wind speed are shown in the second and third rows, respectively.

The SFMR instrument, designed and built by ProSensing, Inc., Amherst, MA [24], is installed on each of two NOAA/Aircraft Operations Center (AOC) WP-3Ds (N42RF and N43RF) aircrafts. The complete description of SFMR instrument and wind speed and rain rate retrievals is given by [45]. According to [45], the AOC SFMR yields wind speed measurements that are overall within 4 m/s rms of the dropwindsonde estimated surface wind and within 5 m/s of the direct 10-m wind speed measurement. A recent study [46] investigated the sensitivity of the SFMR retrieval product's accuracy to small errors introduced by calibration and/or modeling errors. This study showed that deficiencies in the SFMR rain absorption model can produce significant wind speed errors as well as inconsistent results, and developed a new rain absorption model that yields reduced errors in the wind speed retrievals. The SFMR wind retrievals used for this study were reprocessed using rain absorption model given by [46].

The SFMR and ASCAT collocation criteria were the same as the criteria used for the GPS dropsondes, where only ASCAT retrievals that were within 1 h and 5 km from

TABLE I
ASCAT WIND SPEED AND WIND DIRECTION BIAS AND STANDARD DEVIATION DIFFERENCE

Wind Speed Bias (m/s)								
wind speed bin	RSS QuikSCAT		JPL QuikSCAT		NRT QuikSCAT		WindSat	
	CMOD5H	CMOD5N	CMOD5H	CMOD5N	CMOD5H	CMOD5N	CMOD5H	CMOD5N
3-6 m/s	0.02	0.02	0.00	0.00	-0.13	-0.13	-0.27	-0.27
6-10 m/s	-0.10	-0.10	0.15	0.15	-0.09	-0.09	-0.12	-0.13
10-15 m/s	0.26	0.15	0.10	-0.01	-0.19	-0.30	0.27	0.15
>15 m/s	0.08	-0.65	-0.29	-1.02	-0.31	-1.00	0.05	-0.65
Wind Speed STD (m/s)								
wind speed bin	RSS QuikSCAT		JPL QuikSCAT		NRT QuikSCAT		WindSat	
	CMOD5H	CMOD5N	CMOD5H	CMOD5N	CMOD5H	CMOD5N	CMOD5H	CMOD5N
3-6 m/s	1.06	1.06	1.17	1.17	1.25	1.25	1.48	1.48
6-10 m/s	1.01	1.00	1.18	1.17	1.27	1.26	1.43	1.42
10-15 m/s	1.19	1.16	1.43	1.40	1.50	1.46	1.67	1.62
>15 m/s	1.75	1.77	2.14	2.15	2.02	1.95	2.50	2.45
Wind Direction Bias (deg)								
wind speed bin	RSS QuikSCAT		JPL QuikSCAT		NRT QuikSCAT		WindSat	
	CMOD5H	CMOD5N	CMOD5H	CMOD5N	CMOD5H	CMOD5N	CMOD5H	CMOD5N
3-6 m/s	11.3	11.3	6.9	6.8	11.4	11.3	7.8	7.8
6-10 m/s	4.4	4.4	7.5	7.6	8.1	8.1	-0.6	-0.6
10-15 m/s	9.5	9.5	3.5	3.4	5.2	5.2	9.7	9.7
>15 m/s	1.0	1.0	0.2	0.2	0.4	0.4	2.3	2.3
Wind Direction STD (deg)								
wind speed bin	RSS QuikSCAT		JPL QuikSCAT		NRT QuikSCAT		WindSat	
	CMOD5H	CMOD5N	CMOD5H	CMOD5N	CMOD5H	CMOD5N	CMOD5H	CMOD5N
3-6 m/s	24.2	24.2	23.0	22.9	24.8	24.8	38.6	38.7
6-10 m/s	23.1	23.2	22.5	22.4	24.4	24.4	37.0	37.1
10-15 m/s	23.5	23.5	22.0	21.9	23.2	23.2	35.7	25.8
>15 m/s	21.1	21.1	21.7	21.6	22.1	22.1	29.0	29.0

SFMR observations were considered. The SFMR measurements were quality controlled using aircraft parameters such as roll, pitch, and altitude as well as environmental parameters such as air temperature, rain rate, and sea surface temperature. The results of the SFMR and ASCAT wind speed validation are shown in Fig. 11(a) and (b). Similar to the previous analysis, the bias between SFMR and ASCAT wind product was reduced by 0.6 m/s when CMOD5.h was used. However, we did find that SFMR/ASCAT wind speed bias exhibited a linear dependence on the latitude, which we believe is due to uncertainties in the SMFR wind retrievals from errors in the sea surface temperatures utilized in the retrieval process.

During the February 2 flight [Fig. 13(a) and (b)], we were able to measure the radial extent of the 25-m/s wind area in the southwest portion of the storm. SFMR retrievals indicated that the radial extent of the 25 m/s wind area was about 102 km, while analysis of the high wind ASCAT data revealed a radius of 89 km [Fig. 13(b)]. Comparatively, the standard ASCAT wind product did not show any 25-m/s wind speed [Fig. 13(a)]. The GPS dropsonde wind speed and direction measurements are also shown in Fig. 13. The 25-m/s dropsonde wind measurements were coincident with SMFR and high wind ASCAT retrievals and confirmed the validity of the new high wind retrievals obtained by the CMOD5.h GMF.

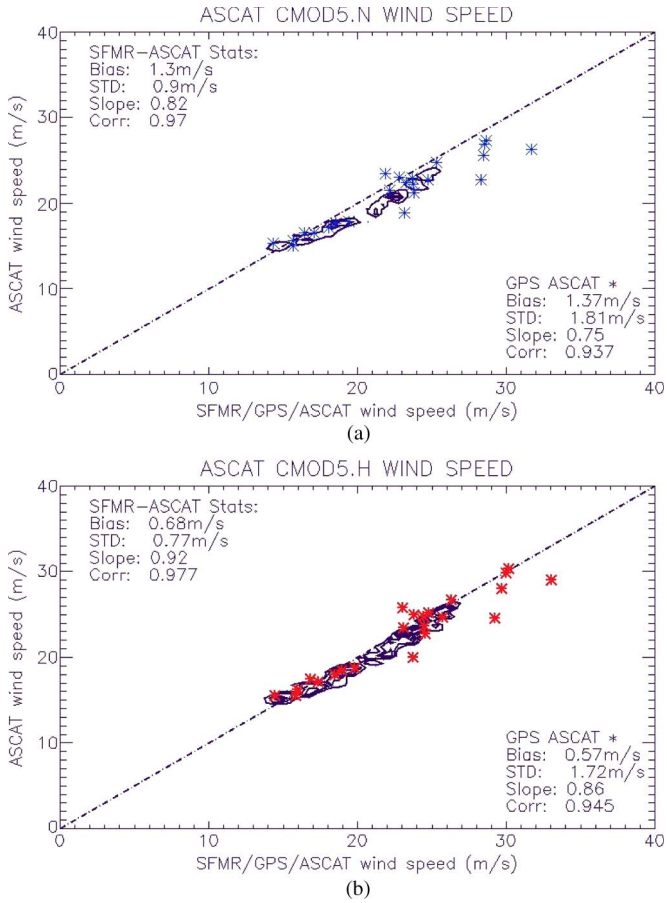

Fig. 11. (a) Standard ASCAT and (b) high wind ASCAT wind speed retrievals versus SFMR and GPS sonde wind speed comparisons.

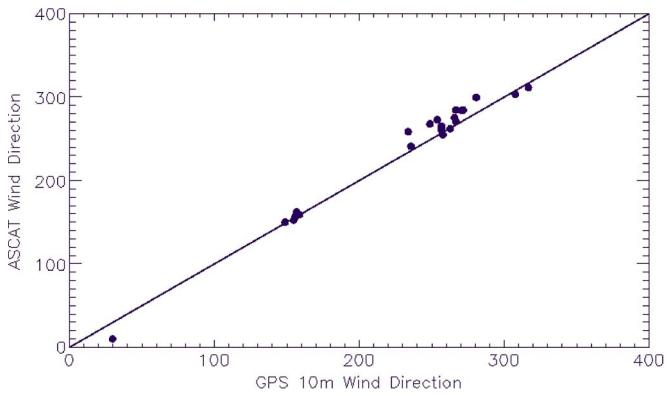

Fig. 12. Comparison of GPS sonde wind direction and ASCAT. The standard deviation was calculated to be 10.1°, and the bias was 5°.

C. High Wind ASCAT Winds and Extratropical Cyclone Observations

To validate the performance of the high wind ASCAT wind retrievals in the extratropical cyclone environment, a study of the wind field distribution during the mature storm stage was conducted. The composites of RSS QuikSCAT, WindSat, and ASCAT wind speeds were created by using a $50^\circ \times 50^\circ$ box that was divided into 400 lat/lon grid cells, which resulted in an approximate grid resolution of 12.5 km. The grid box was centered on the storm center locations obtained from OPC's extratropical cyclone best track storm file [47]. A mean wind field of extratropical cyclones that reached HF wind status during the 2007–2009 North Pacific winter seasons in the North Pacific was calculated from RSS QuikSCAT standard and high wind ASCAT composites and are shown in Fig. 14(a)–(c), respectively. The average wind speed field from WindSat wind vector retrievals was found to agree with QuikSCAT, and it is not presented in the plots. The QuikSCAT mean wind field reveals an asymmetric wind field structure, with the strongest winds concentrated on the southeast side with respect to storm motion direction [Fig. 14(a)]. The average wind speed maximum falls in the storm force category and is depicted by the orange color. The area of strongest winds spans ∼500 km in longitudinal direction and ∼400 km in latitudinal direction. Both the standard and high wind ASCAT products are generally in good agreement for low to moderate wind speeds. However, while the standard ASCAT reveals no storm force mean winds, the high wind ASCAT composites do show storm force wind area that correlates well with QuikSCAT composite. The total area of strongest winds in the ASCAT composites is about 20% less than that of QuikSCAT, which can be attributed to the lower ASCAT wind retrievals as well as the smaller number of observations due to the smaller swath coverage.

Fig. 15 shows the frequency of gale, storm, and HF wind speed occurrences within the composite grids. The QuikSCAT plots [Fig. 15(a)] reveal that there is greater than 20% probability of encountering gale force winds within a radius of 1000 km from the storm center for any time and direction. The storm force winds can span beyond 500 km from the storm center, with the leading edge opening in the direction of storm motion. The HF winds are concentrated within a 500 km radius, south–southeast from the center relative to the storm motion direction. The significant improvement between the operational [Fig. 15(b)] and high wind ASCAT retrievals [Fig. 15(c)] is mainly noticeable within the storm force wind warning category (24–31.5 m/s). The spatial distribution of storm force winds in the high wind ASCAT product is much closer to that of QuikSCAT, and the probability of storm force wind detection rises from 12% to more than 20% within the southwest corner of the storm for the operational and high wind ASCAT, respectively. For gale force winds, all three retrievals, namely, QuikSCAT, standard ASCAT, and high wind ASCAT, exhibit very similar frequency and spatial distributions. The detection of HF winds with high wind ASCAT has increased by 24% with respect to standard ASCAT when compared to QuikSCAT HF detection capabilities.

V. Summary and Conclusion

The operational use of satellite OSVW observations has advanced considerably over the past decade. OSVW data from research (QuikSCAT and WindSat) and operational (ASCAT) satellite systems are now depended upon and utilized daily by operational weather forecast and warning centers around the world. With the oceans comprising over 70% of the Earth's surface, the impacts of remotely sensed OSVW data have been significant in meeting societal needs for weather and

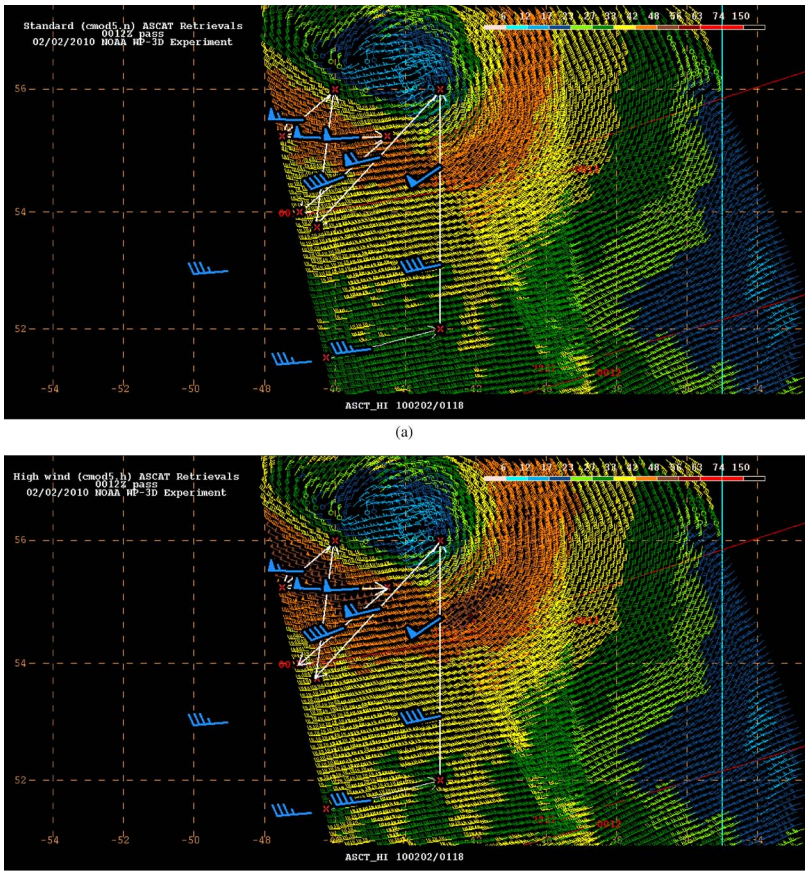

Fig. 13. NOAA WP-3D Ocean Winds Experiment flight track over extratropical storm in North Atlantic on February 2, 2010, coincident with ASCAT 0012Z and 2339Z passes. (a) Standard (CMOD5.n) and (b) high wind (CMOD5.h) ASCAT wind retrievals with GPS dropsonde 10-m neutral wind measurements (blue wind barbs) overlayed.

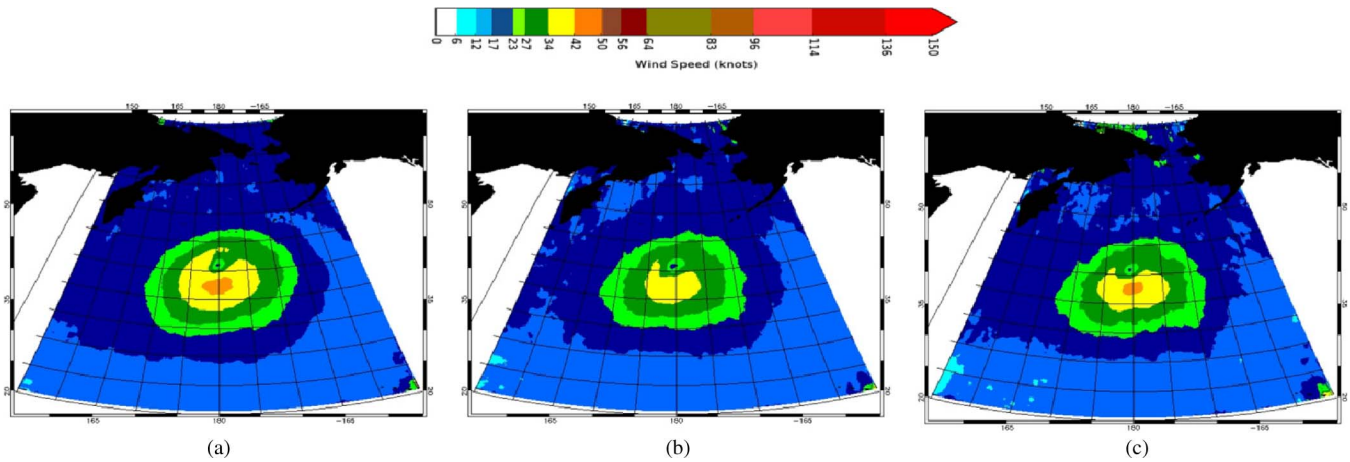

Fig. 14. Mean wind speed composite of 2007–2009 winter seasons of (a) QuikSCAT, (b) standard ASCAT, and (c) high wind ASCAT. The color code represents wind speed in knots.

water information and in supporting the nation's commerce with information for safe, efficient, and environmentally sound transportation and coastal preparedness. Within NOAA's NWS, the use of OSVW encompasses the warning, analysis, and forecasting missions associated with TCs, extratropical cyclones, fronts, localized coastal wind events (i.e., gap winds), and the forecast of sea conditions driven by winds. The advent of ASCAT into NWS operations helped partially fill the immense void in ocean wind measurements that resulted from the loss of QuikSCAT. However, the reduced sensitivity of ASCAT winds above > 15 m/s limited its usefulness to support NWS wind warning and forecasting products and services.

In a comparison of ASCAT σ_0 measurements, the σ_0 values predicted by the CMOD5.n GMF and the high-wind-speed

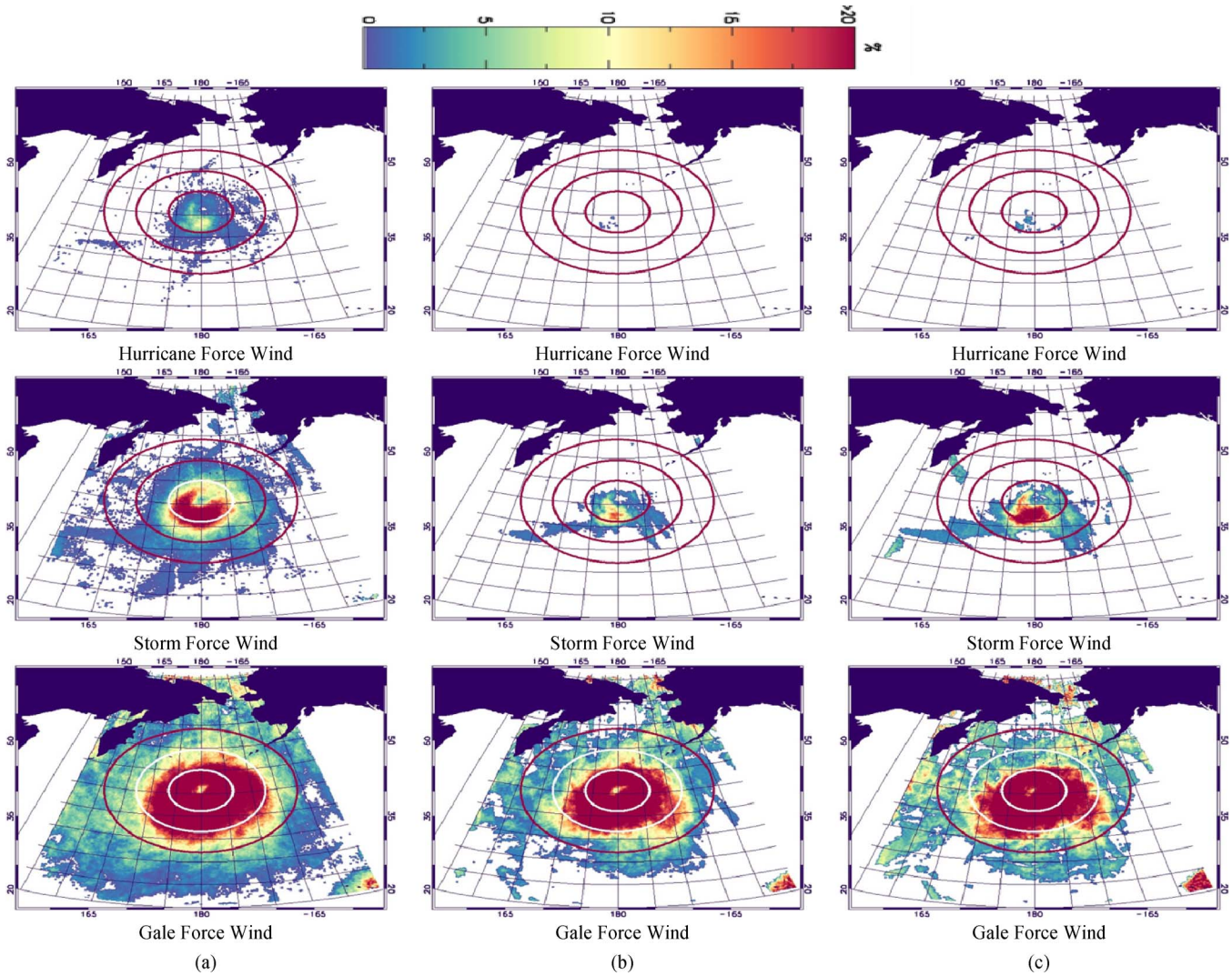

Fig. 15. Frequency of each wind warning category of (a) QuikSCAT, (b) standard ASCAT, and (c) high wind ASCAT. The color code represents relative percentage of frequency.

retrievals from QuikSCAT revealed that ASCAT σ_0 measurements exhibited sensitivity to the higher wind speeds that was not being represented in CMOD5.n. This suggested that the ASCAT high-wind-speed retrieval performance could potentially be improved. However, the lack of high-wind-speed measurements to use as a ground truth for a robust empirical development of an improved high-wind-speed GMF required development of a novel technique of using high-resolution high-wind-speed aircraft scatterometer measurements to develop the high-wind-speed portion of the high wind ASCAT GMF called CMOD5.h.

The CMOD5.h has been implemented in the KNMI developed ASCAT wind processor that was adapted to run at NOAA. One year of ASCAT data reprocessed with both CMOD5.n and CMOD5.h was produced for validation analysis. Comparisons were done using collocated three QuikSCAT and RSS WindSat wind products. Overall, the negative bias between standard ASCAT and QuikSCAT and WindSat winds was reduced for all winds greater than 15 m/s by 0.6 m/s while standard deviation remained about the same. Since it was determined that the standard ASCAT wind directional retrieval accuracy was very good, the goal of preserving it was achieved with CMOD5.h model too. For weather forecasting and warning products, the high wind ASCAT product shows the most improvement in gale force and storm force wind categories and substantially increases the utility of ASCAT winds to support NWS operations. Data collected from several NOAA P-3 aircraft flights in extratropical cyclones coincident with ASCAT overpasses also validated the improved high wind speeds retrieved using the CMOD5.h GMF. The ASCAT wind speeds retrieved using the CMOD5.h GMF not only agreed better than the standard ASCAT wind products but also better captured the actual 25 m/s wind radii extent as measured by SFMR.

The high wind ASCAT wind product processing is currently running in parallel with the operational (original) wind products. Winds are provided to OPC and NHC in a NRT basis, and a graphical display of both standard ASCAT (run with CMOD5.n) and high wind ASCAT (run with CMOD5.h) can be found at http://manati.star.nesdis.noaa.gov/datasets/ASCATData.php/.

REFERENCES

[1] J. Figa-Saldana, J. J. W. Wilson, E. Attema, R. Gelsthorpe, M. R. Drinkwater, and A. Stoffelen, "The Advanced Scatterometer (ASCAT) on the meteorological operational (MetOp) platform: A follow on for European wind scatterometers," *Can. J. Remote Sens.*, vol. 28, no. 3, pp. 404–412, Jun. 2002.

[2] J. J. W. Wilson, C. Anderson, M. A. Baker, H. Bonekamp, J. Figa Saldana, R. G. Dyer, J. A. Lerch, G. Kayal, R. V. Gelsthorpe, M. A. Brown, E. Schied, S. Schutz-Munz, F. Rostan, E. W. Pritchard, N. G. Wright, D. King, and U. Onel, "Radiometric calibration of the advanced wind scatterometer radar ASCAT carried onboard the MetOp-A satellite," *IEEE Trans. Geosci. Remote Sens.*, vol. 48, no. 8, pp. 3236–3255, Aug. 2010.

[3] *ASCAT Product Guide. Ref EUM/OPS-EPS/MAN/04/0028*, Issue: v2C, EUMETSAT, Darmstadt, Germany, Apr. 8, 2008. [Online]. Available: http://oiswww.eumetsat.org/WEBOPS/eps-pg/ASCAT/ASCAT-PG-0TOC.htm

[4] A. Verhoef, J. Vogelzang, J. Verspeek, and A. Stoffelen, *AWDP User Manual and Reference Guide*. De Bilt, The Netherlands: KNMI, version 1.1, 2010, NWPSAF-KN-UD-005, EUMETSAT, 2010. [Online]. Available: http://www.knmi.nl/publications/fulltexts/awdp_um_and_rg_v1_1.pdf

[5] M. Portabella and A. Stoffelen, "On Bayesian scatterometer wind inversion," *IEEE Trans. Geosci. Remote Sens.*, vol. 44, no. 6, pp. 1523–1533, Jun. 2006.

[6] J. Verspeek, A. Stoffelen, M. Portabella, H. Bonekamp, C. Anderson, and J. Figa-Saldana, "Validation and calibration of ASCAT using CMOD5.n," *IEEE Trans. Geosci. Remote Sens.*, vol. 48, no. 1, pp. 386–395, Jan. 2010.

[7] S. Soisuvarn, Z. Jelenak, P. S. Chang, Q. Zhu, and G. Sindic-Rancic, "Validation of NOAA's near real-time ASCAT ocean vector winds," in *Proc. IGARSS*, 2008, pp. I-118–I-121.

[8] F. J. Wentz and D. K. Smith, "A model function for the ocean-normalized radar cross section at 14 GHz derived from NSCAT observations," *J. Geophys. Res.*, vol. 104, no. C5, pp. 11 499–11 514, May 15, 1999.

[9] D. E. Fernandez, J. R. Carswell, S. Frasier, P. S. Chang, P. G. Black, and F. D. Marks, "Dual-polarized C- and Ku-band ocean backscatter response to hurricane-force winds," *J. Geophys. Res.*, vol. 111, no. C8, pp. C08013-1–C08013-17, 2006.

[10] N. Bowditch, *The American Practical Navigator*. St. Louis, MO: Nat. Imagery Mapping Agency Publ., 2005, p. 879. [Online]. Available: http://msi.nga.mil/NGAPortal/MSI.portal?_nfpb=true&_pageLabel=msi_portal_page_62&pubCode=0002

[11] J. Sienkiewicz, K. Ahmad, and J. Von-Ahn, Preliminary assessment of the utility of ASCAT ocean surface wind vector retrievals (OSVW) at the Ocean Prediction Center (OPC), NOAA Ocean Predict. Center, Camp Springs, MD, technical report. [Online]. Available: ftp://ftp.mpc.ncep.noaa.gov/reports/OPC_ASCAT_evaluation.pdf

[12] H. Cobb, R. Knabb, P. S. Chang, and Z. Jelenak, "Preliminary assessment of the utility of ASCAT wind vector retrievals at the Tropical Prediction Center/National Hurricane Center," in *Proc. Preprints 28th Conf. Hurricanes Tropical Meteorol.*, Orlando, FL, 2008.

[13] P. K. Taylor, E. C. Kent, M. J. Yelland, and B. I. Moat, "The accuracy of marine surface winds from ships and buoys," in *Proc. CLIMAR, WMO Workshop Adv. Marine Climatol.*, Vancouver, BC, Canada, Sep. 8-15, 1999, pp. 59–68.

[14] V. J. Cardone, E. A. Ceccacci, A. T. Cox, and J. G. Greenwood, "Accuracy of scatterometer winds assessed from *in-situ* measured wind data up to 32 m/s," presented at the Meeting American Geophysical Union, Washington, DC, 2000, Paper OS52A-03.

[15] V. R. Swail and A. T. Cox, "On the use of NCEP/NCAR reanalysis surface marine wind fields for a long term North Atlantic wave hindcast," *J. Atmos. Ocean. Technol.*, vol. 17, no. 4, pp. 532–545, Apr. 2000.

[16] M. Freilich and R. S. Dunbar, "Derivation of satellite wind model functions using operational surface wind analyses: An altimeter example," *J. Geophys. Res.*, vol. 98, no. C8, pp. 14 633–14 649, Aug. 1993.

[17] P. S. Callahan, *QuikSCAT Science Data Product User's Manual, Overview and Geophysical Data Products*. Pasadena, CA: JPL, V3.0, D-18053-RevA, 2006. [Online]. Available: ftp://podaac.jpl.nasa.gov/OceanWinds/quikscat/L2B/v2/docs/QSUG_v3.pdf

[18] L. Ricciardulli and F. J. Wentz, "Reprocessed QuikSCAT (V04) wind vectors with Ku-2011 geophysical model function," Remote Sens. Syst., Santa Rosa, CA, Tech. Rep. 043011, 2011.

[19] D. B. Chelton and M. H. Freilich, "Scatterometer-based assessment of 10-m wind analyses from the operational ECMWF and NCEP numerical weather prediction models," *Mon. Weather Rev.*, vol. 133, no. 2, pp. 409–429, Feb. 2005.

[20] N. Ebuchi, "Evaluation of wind vectors observed by QuikSCAT/SeaWinds using ocean buoy data," *J. Atmos. Ocean. Technol.*, vol. 19, no. 12, pp. 2049–2062, Dec. 2002.

[21] M. Bourassa, D. Legler, J. O'Brien, and S. Smith, "SeaWinds validation with research vessels," *J. Geophys. Res.*, vol. 108, no. C2, pp. 1–16, 2003.

[22] K.-H. Chou, C.-C. Wu, P.-H. Lin, and S. Majumdar, "Validation of QuikSCAT wind vectors by dropwindsonde data from Dropwindsonde Observations for Typhoon Surveillance Near the Taiwan Region (DOTSTAR)," *J. Geophys. Res.*, vol. 115, pp. D02109-1–D02109-11, Jan. 2010.

[23] T. Chu, "Operation and improvement of the IWRAP airborne Doppler radar/scatterometer," M.S. thesis, Univ. Massachusetts Amherst, Amherst, MA, 2008.

[24] M. A. Goodberlet and J. B. Mead, "Two-load radiometer precision and accuracy," *IEEE Trans. Geosci. Remote Sens.*, vol. 44, no. 1, pp. 58–67, Jan. 2006.

[25] T. F. Hock and J. L. Franklin, "The NCAR GPS dropwindsonde," *Bull. Amer. Meteorol. Soc.*, vol. 80, pp. 407–420, 1999.

[26] X. Yuan, "High-wind-speed evaluation in the Southern Ocean," *J. Geophys. Res.*, vol. 109, no. D13, pp. D13101-1–D13101-10, 2004.

[27] B. W. Stiles and S. H. Yueh, "Impact of rain on spaceborne Ku-band wind scatterometer data," *IEEE Trans. Geosci. Remote Sens.*, vol. 40, no. 9, pp. 1973–1983, Sep. 2002.

[28] A. Bentamy, D. Croize-Fillon, and C. Perigaud, "Characterization of ASCAT measurements based on buoy and QuikSCAT wind vector observations," *Ocean Sci.*, vol. 4, no. 4, pp. 265–274, 2008.

[29] J.; Patoux and R. C. Foster, "Cross-validation of scatterometer measurements via sea-level pressure retrieval," *IEEE Trans. Geosci. Remote Sens.*, vol. 50, no. 7, pp. 2507–2517, Jul. 2012.

[30] T. Meissner and F. J. Wentz, "Wind vector retrievals under rain with passive satellite microwave radiometers," *IEEE Trans. Geosci. Remote Sens.*, vol. 47, no. 9, pp. 3065–3083, Sep. 2009.

[31] T. Meissner, L. Ricciardulli, and F. J. Wentz, "Wind measurements from active and passive microwave sensors: High winds and winds in rain," presented at the Presented Int. Scientific Radio Union (URSI) Commission F Microwave Signatures Meeting, Florence, Italy, 2010.

[32] P. S. Chang, Z. Jelenak, J. M. Sienkiewicz, R. Knabb, M. J. Brennan, D. G. Long, and M. Freeberg, "Operational use and impact of satellite remotely sensed ocean surface vector winds in the marine warning and forecasting environment," *Oceanography*, vol. 22, no. 2, pp. 194–207, Jun. 2009.

[33] A. E. Long, "Towards a C-Band radar sea echo model for the ERS-1 scatterometer," in *Proc. 3rd Int. Colloq. Spectral Signatures Objects Remote Sens.*, Les Arcs, France, 1984, pp. 29–34.

[34] A. Stoffelen and D. Anderson, "Scatterometer data interpretation: Transfer function estimation and validation," *J. Geophys. Res.*, vol. 102, no. C3, pp. 5767–5780, 1997.

[35] J. R. Carswell, W. J. Donnelly, R. E. McIntosh, M. A. Donelan, and D. C. Vandemark, "Analysis of C and Ku band ocean backscatter measurements under low-wind conditions," *J. Geophys. Res.*, vol. 104, no. C9, pp. 20 687–20 701, Sep. 1999.

[36] W. J. Donnelly, J. R. Carswell, R. E. McIntosh, P. S. Chang, J. Wilkerson, F. Marks, and P. G. Black, "Revised ocean backscatter models at C and Ku-band under high-wind conditions," *J. Geophys. Res.*, vol. 104, no. C5, pp. 11 485–11 497, May 1999.

[37] H. Hersbach, A. Stoffelen, and S. Haan de, "An improved C-band scatterometer ocean geophysical model function: CMOD5," *J. Geophys. Res.*, vol. 112, no. C3, pp. C03006-1–C03006-18, Mar. 2007.

[38] H. Hersbach, "CMOD5.N: A C-band geophysical model function for equivalent neutral wind," ECMWF, Reading, U. K., Tech. Memo. 554, 2008.

[39] S. Abdalla and H. Hersbach, The technical support for global validation of ERS Wind and Wave Products at ECMWF (April 2004–June 2007), ECMWF, Reading, U. K., Final rep. for ESA contract 18212/04/I-LG. [Online]. Available: http://www.ecmwf.int/publications/library/ecpublications/pdf/esa/ESAabdallahersbach182122007.pdf

[40] M. Portabella and A. Stoffelen, Development of a global scatterometer validation and monitoring, Roy. Netherlands Meteorol. Inst., De Bilt, The Netherlands. [Online]. Available: http://www.knmi.nl/publications/

[41] H. Hersbach, "Comparison of C-band scatterometer CMOD5.n equivalent neutral winds with ECMWF," *J. Atmos. Ocean. Technol.*, vol. 27, no. 4, pp. 721–736, Apr. 2010.

[42] D. E. Fernandez, E. M. Kerr, A. Castells, J. R. Carswell, S. J. Frasier, P. S. Chang, P. G. Black, and F. D. Marks, "IWRAP: The imaging wind and rain airborne profiler for remote sensing of the ocean and the atmospheric boundary layer within tropical cyclones," *IEEE Trans. Geosci. Remote Sens.*, vol. 43, no. 8, pp. 1775–1787, Aug. 2005.

[43] E. Rodriguez and S. Veleva, "The high wind speed model function from space," in *Proc. NASA Ocean Vector Wind Sci. Team Meeting*,

Boulder, CO, May 18–20, 2009. [Online]. Available: http://coaps.fsu.edu/scatterometry/meeting/docs/2009_may/calval/rodriguez.pdf
[44] A. Stoffelen, "Scatterometry," M.S. thesis, Univ. Utrecht, Utrecht, The Netherlands, 1998.
[45] E. W. Uhlhorn, P. G. Black, J. L. Franklin, M. Goodberlet, J. Carswell, and A. S. Goldstein, "Hurricane surface wind measurements from an operational stepped frequency microwave radiometer," *Mon. Weather Rev.*, vol. 135, no. 9, pp. 3070–3085, Sep. 2007.
[46] J. Carswell, Z. Jelenak, P. S. Chang, S. Frasier, and D. Esteban-Fernandez, "Improved hurricane-force surface winds and rain rate retrievals with the step frequency microwave radiometer," *IEEE Trans. Geosci. Remote Sens.*, submitted for publication.
[47] Z. Jelenak, K. Ahmad, J. Sienkiewicz, and P. S. Chang, "A statistical study of wind field distribution within extra-tropical cyclones in North Pacific ocean from 7-years of QuikSCAT wind data," in *Proc. IEEE IGARSS*, 2009, pp. I-104–I-107.

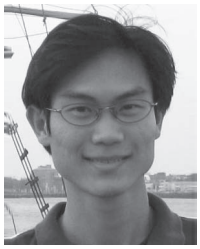

Seubson Soisuvarn (S'02–M'07) received the B.Eng. degree from Kasetsart University, Bangkok, Thailand, in 1998 and the M.S.E.E. and Ph.D. degrees in electrical engineering from the University of Central Florida, Orlando, in 2001 and 2006, respectively.

From 2001 to 2006, he was with the Central Florida Remote Sensing Laboratory, where his primary research focused on combined active and passive microwave remote sensing of ocean surface vector winds. Since 2006, he has been a UCAR Visiting Scientist with the Center for Satellite Applications and Research, National Environmental Satellite, Data, and Information Service, National Oceanic and Atmospheric Administration (NOAA). He has worked on calibration and validation of ASCAT wind scatterometer and geophysical model function development to improve NOAA high wind products. His current research is focused on calibration and validation of Oceansat-2 scatterometer and ocean vector wind retrieval algorithm development.

Zorana Jelenak (S'97–M'04) received the Ph.D. degree in physics from Waikato University, Hamilton, New Zealand, in 2000.

Her interests are in ocean surface wind vector measurements from active and passive microwave measurements and its applicability in an operational near-real-time environment, retrieval algorithm development, model function development, advanced statistical analysis, and error analysis for improved algorithm characterization. She joined Ocean Winds Team at NOAA/NESDIS/ORA as a UCAR Visiting Scientist in March 2001. She is a member of the NASA Ocean Surface Winds Science Team, NOAA's EDR algorithm lead for AMSR-2 radiometer, and a member of NASA CYGNSS Science Team.

Paul S. Chang (S'87–M'90) received the B.S. degree in electrical engineering from Union College, Schenectady, NY, in 1988 and the Ph.D. degree in electrical engineering from the University of Massachusetts, Amherst, in 1994.

Since 1994, he has been a Research Physical Scientist with the Center for Satellite Applications and Research, National Environmental Satellite, Data, and Information Service (NESDIS), National Oceanic and Atmospheric Administration (NOAA), where he leads the NESDIS Ocean Winds Science Team. His current activities include research and development in active and passive microwave remote sensing of the ocean surface, with emphasis on retrieval of the ocean surface wind field. Wind retrieval algorithm improvements and new product developments are pursued through the analyses of satellite and aircraft microwave remote sensing data. An emphasis is placed on transitioning research results into operational use, which involves cooperative relationships with the operational facets of NESDIS and with the National Weather Service, a primary end user of these data. He is a member of the NASA Ocean Surface Winds Science Team, a member of the NASA CYGNSS Science Team, and the Project Scientist for NOAA's GCOMW1 project. His current efforts are focused on working with international partners on the MetOp, Oceansat-2, and GCOM-W missions in addition to planning and risk reduction activities for future ocean vector wind missions.

Suleiman O. Alsweiss (S'05–M'11) received the B.E. degree in electrical engineering from the Princess Sumaya University for Technology, Amman, Jordan, in 2004 and the M.S. and Ph.D. degrees in electrical engineering from the University of Central Florida (UCF), Orlando, in 2007 and 2011, respectively.

He joined the Central Florida Remote Sensing Laboratory, UCF, in January 2006 as a Research Assistant, where his primary research focused on active and passive microwave remote sensing of ocean surface vector winds (OVW). In November 2011, he joined the OVW team within NOAA, where he continued his work on developing and validating satellite ocean vector winds.

Qi Zhu received the M.S. degree in information systems from Northeastern University, Boston, MA, in 2001.

Since February 2002, she has been with the National Oceanic and Atmospheric Administration (NOAA), and she is currently a Scientific Programmer with the Satellite Ocean Surface Winds group in STAR/NESDIS/NOAA.